Research Square

Preprints are preliminary reports that have not undergone peer review.
They should not be considered conclusive, used to inform clinical practice,
or referenced by the media as validated information.

A computational method based on Bicubic spline Interpolation for (2+1) dimensional Sobolev and generalize BBMB models

Shams Ul Arifeen

aarrifeen@gmail.com

National University of Science and Technology https://orcid.org/0000-0002-9222-7610

Research Article

Keywords: Sobolev, bicubic B-spline, BBM

Posted Date: November 2nd, 2026

DOI: https://doi.org/10.21203/rs.3.rs-11528642/v1

License: This work is licensed under a Creative Commons Attribution 4.0 International License.
Read Full License

Additional Declarations: The authors declare no competing interests.

A computational method based on Bicubic spline Interpolation for (2+1) dimensional Sobolev and generalize BBMB models

Shams Ul Arifeen[1*] and Abdul Ghafoor[2]

[1*]Department of Mathematics, School of Natural Sciences, National University of Sciences and Technology, H12, Islamabad, 44000, , Pakistan.

[2]Institute of Numerical Sciences, Kohat University of Science and Technology, Kohat, 26000, KP, Pakistan.

*Corresponding author(s). E-mail(s): aarrifeen@gmail.com;
Contributing authors: abdulghafoor@kust.edu.pk;

Abstract

This paper presents a computational study of the two-dimensional Sobolev and nonlinear generalized Benjamin-Bona-Mahony-Burgers (NGBBMB) equations, which arise in fluid-flow and wave-propagation models. An efficient numerical method based on bicubic spline interpolation is proposed to approximate their solutions. Becouse of two spatial and time variables, first we descritize temporal part using finite difference approche while spatial part is approximated by bicubic spline technique. With this strategy, two-dimensional PDEs are transformed into systems of algebraic equations, and a collocation approach is employed to determine the spline coefficients. The numerical results demonstrate that the (1+2) dimensional bicubic spline method is robust and efficient for solving two-dimensional linear and nonlinear PDEs. The $\boldsymbol{L_2}$ and $\boldsymbol{L\infty}$ norms are computed to validate the proposed scheme, confirming its accuracy and effectiveness. The graphical solution profiles demonstrate close agreement between the exact and approximate solutions for all considered problems

Keywords: Sobolev, bicubic B-spline, BBM

MSC Classification: 65D07 , 65M06 , 35G20

1 Introduction

Mathematical equations provide an effective framework for modelling physical processes and predicting their future behaviour. Over the past two decades, partial differential equations (PDEs) have been extensively employed to investigate various natural phenomena. Nonlinear PDEs and Sobolev-type equations arise in numerous fields, including fluid flow through fractured rocks, thermodynamics, soil mechanics, finance, and heat conduction. In particular, nonlinear PDEs provide more realistic descriptions of complex physical processes. The current work considers the following two-dimensional PDE [1]:

$$\chi_t - \Delta\chi_t - \sigma_1\Delta\chi + \sigma_2\nabla\cdot\chi + \sigma_3\nabla\cdot(\chi\nabla\chi) + \sigma_4\chi^2 = \sigma_5\nabla\cdot\big(E(\chi)\big) + f(\mathbf{x},t), \quad \mathbf{x}\in\chi, \quad t>0, \tag{1}$$

where for simplicity $\mathbf{x} = (\xi,\eta)$. The associated initial and boundary conditions are

$$\begin{cases} \chi(\mathbf{x},0) = \eta_1(\mathbf{x}), & \mathbf{x}\in\chi, \\ \chi(\mathbf{x},t) = \eta_2(\mathbf{x},t), & \mathbf{x}\in\partial\chi, \quad t>0. \end{cases} \tag{2}$$

Here, $\chi = \chi(\mathbf{x},t)$, $E(\chi)$ is a nonlinear function, Δ and ∇ are the two-dimensional Laplacian and gradient operators, respectively, and $\sigma_l \in \mathbb{R}, \quad l = 1,\ldots,5$.

For $\sigma_1 = 1, \sigma_2 = \sigma_3 = \sigma_4 = \sigma_5 = 0$, equation (1) reduces to the linear Sobolev equation

$$\chi_t - \Delta\chi_t - \Delta\chi = f(\mathbf{x},t), \quad \mathbf{x}\in\chi, \quad t>0. \tag{3}$$

For $\sigma_1 = \sigma_2 = \sigma_5 = 0, \sigma_3 = -1, \sigma_4 = \pi^2$, equation (1) reduces to the nonlinear Sobolev equation

$$\chi_t - \Delta\chi_t - \nabla\cdot(\chi\nabla\chi) + \pi^2\chi^2 = f(\mathbf{x},t), \quad \mathbf{x}\in\chi, \quad t>0. \tag{4}$$

For $\sigma_1 = \sigma_2 = \sigma_5 = 1, \sigma_3 = \varsigma_4 = 0$, equation (1) reduces to the nonlinear generalized (NGBBMB) equation

$$\chi_t - \Delta\chi_t - \Delta\chi + \nabla\cdot\chi = \nabla\cdot\big(E(\chi)\big) + f(\mathbf{x},t), \quad \mathbf{x}\in\chi, \quad t>0. \tag{5}$$

Sobolev-type equations arise in various areas of applied sciences and engineering, particularly in the modelling of nonlinear wave propagation and convection-dominated processes. Numerous analytical, semi-analytical, and numerical methods have been developed for solving differential equations (DEs). However, closed-form solutions to nonlinear DEs are often difficult or impossible to obtain, particularly for complex initial and boundary conditions. Semi-analytical methods may also involve lengthy derivations and can become computationally demanding. Consequently, numerical methods play an essential role in approximating solutions to complex differential equations. Moreover, advances in digital computing have facilitated the implementation of efficient numerical schemes capable of providing accurate and reliable solutions. Numerical methods based on finite elements have been reported in the literature,

including semidiscrete and fully discrete local discontinuous Galerkin methods, discontinuous Galerkin space-time, characteristic finite-element methods, split least-squares characteristic mixed finite-element methods, and modified weak Galerkin methods based on global weak gradients [2–5]. Finite difference method has been employed for Sobolev equations involving convection terms [6]. In recent studies, weak Galerkin and two-grid finite-volume methods have been introduced to reduce computational costs while preserving satisfactory accuracy [7, 8]. In addition, Haar-wavelet methods combined with finite-difference schemes have been applied to two-dimensional Sobolev equations, whereas Hermite-wavelet method has been used to approximate solutions to multidimensional problems [1, 9]. Haar wavelets are particularly attractive because of their compact support, simple structure, and multiresolution properties, which facilitate implementation and enable efficient representation of local solution behaviour. A mixed Lucas-Fibonacci polynomial scheme has also been proposed, in which temporal derivatives are discretized using finite differences and spatial derivatives are approximated through polynomial expansions [10].
The generalized Benjamin-Bona-Mahony-Burgers (GBBMB) equation is an important model for describing long surface waves in liquids, hydromagnetic waves in cold plasma, acoustic-gravity waves in compressible fluids, and acoustic waves in anharmonic crystals [11, 12]. Various numerical techniques, including radial basis function and Haar-wavelet methods, have been developed for solving the BBM and generalized BBM-Burgers equations [1, 11].

The objective of the present study is to employ bicubic spline interpolation to approximate solutions to the (1+2) dimensional Sobolev and GBBMB equations. The salient features of spline are local compact support system and differentiability due to polynomail nature. To the best of our knowledge, bicubic spline methods have not previously been applied to two-dimensional nonlinear problems, and only limited work has been published on this topic. This research gap motivates the application of the proposed method to the problem defined in (1). Existing studies involving bicubic splines have focused on linear problems. For example, Nur Nadiah et al. applied bicubic B-splines to the heat and Laplace equations [13, 14]. Similarly, Arshad et al. developed an efficient bicubic B-spline method for the Laplace equation [15], whereas Rohila et al. considered the advection-diffusion equation. Additional related studies are presented in [16–18] and the references therein.
The distribution of this study is organized as follows. Section 2 presents the basic formulation of bicubic splines and their application to function approximation. Section 3 describes the time discretization along with convergence and stablity where in Section 4, solution methodology for the (1+2) dimensional Sobolev and GBBMB equations is discussed. The stability analysis of the proposed method is presented in Section 5. Section 6 provides several numerical examples to demonstrate the accuracy, efficiency, and robustness of the method. Finally, concluding remarks are given in Section 7.

2 Derivation of the Scheme

Let $\chi = [a, b] \times [c, d]$ be a rectangular spatial domain and $[0, T]$ be time domain and the corresponding uniform mesh sizes are defined as:

$$\Delta\xi = \frac{b-a}{m}, \qquad \Delta\eta = \frac{d-c}{m}, \qquad \Delta t = \frac{T}{n},$$

where for uniform spatial mesh size $h = \Delta\xi = \Delta\eta$ and T be the final time.

$$\chi(\xi, \eta, t) = \sum_{s=-1}^{m+1} \sum_{\varsigma=-1}^{m+1} \zeta_{s,\varsigma}(t)\Phi_{s,\varsigma}(\xi, \eta), \tag{6}$$

where $\zeta_{s,\varsigma}$ are unknown parameters to be computed and $\Phi_{s,\varsigma}(\xi, \eta)$ be the cubic B-spline function , which can be expressd in simplified form $\Phi_{s,\varsigma}(\xi, \eta) = \Phi_s(\xi)\Phi_\xi(\eta)$ and $\Phi_s(\xi)$ is defined as [19]:

$$\Phi_s(\xi) = \frac{1}{h^3}\begin{cases} (\xi - \xi_{s-2})^2, & \xi_{s-2} \le \xi < \xi_{s-1}, \\ -3(\xi - \xi_{s-1})^3 + h^3 - 3h(\xi - \xi_{s-1})^2 + 3h^2(\xi - \xi_{s-1}), & \xi_{s-1} \le \xi < \xi_s, \\ -3(\xi_{s+1} - \xi)^3 + h^3 - 3h(\xi_{s+1} - \xi)^2 + 3h^2(\xi_{s+1} - \xi), & \xi_s \le \xi < \xi_{s+1}, \\ (\xi_{s+2} - \xi)^3, & \xi_{s+1} \le \xi < \xi_{s+2}, \\ 0, & \text{else.} \end{cases} \tag{7}$$

Similarly , the same defintion is applied for $\Phi_s(\eta)$. The splines $\Phi_{s-1}, \Phi_s, \Phi_{s+1}$ and Φ_{s+2} have zero contribution outside of the interval $[\xi_s, \xi_{s+1}]$. For one dimentional, the approximaion in local element form is expressed as:

$$\chi(\xi, t) = \sum_{j=s-1}^{s+2} \zeta_j(t)\Phi_j(\xi). \tag{8}$$

Expressing χ, χ' and χ'' at the nodal points are as follows:

$$\begin{cases} \chi_s = \zeta_{s-1} + 4\zeta_s + \zeta_{s+1}, \\ \chi'_s = \dfrac{3}{h}(\zeta_{s+1} - \zeta_{s-1}), \\ \chi''_s = \dfrac{6}{h^2}(\zeta_{s+1} - 2\zeta_s + \zeta_{s-1}), \qquad s = 0, 1, \ldots, m. \end{cases} \tag{9}$$

Now extend the same concept for two dimensional approxlimatons and express χ, χ_ξ, χ_η, $\chi_{\xi\xi}$ and $\chi_{\eta\eta}$ at the nodal point are as follows:

$$\chi_{s,\varsigma} = \zeta_{s-1,\varsigma-1} + 4\zeta_{s-1,\varsigma} + \zeta_{s-1,\varsigma+1} + 4\zeta_{s,\varsigma-1} + 16\zeta_{s,\varsigma} + 4\zeta_{s,\varsigma+1} + \zeta_{s+1,\varsigma-1} + 4\zeta_{s+1,\varsigma} + \zeta_{s+1,\varsigma+1}. \tag{10}$$

$$\begin{aligned}
\frac{\partial \chi_{s,\varsigma}}{\partial \xi} &= -\frac{3}{h}\Big(\zeta_{s-1,\varsigma-1} + 4\zeta_{s-1,\varsigma} + \zeta_{s-1,\varsigma+1} - \zeta_{s+1,\varsigma-1} - 4\zeta_{s+1,j} - \zeta_{s+1,\varsigma+1}\Big),\\
\frac{\partial \chi_{s,\varsigma}}{\partial \eta} &= -\frac{3}{h}\Big(\zeta_{s-1,\varsigma-1} - \zeta_{s-1,\varsigma+1} + 4\zeta_{s,\varsigma-1} - 4\zeta_{s,\varsigma+1} + \zeta_{s+1,\varsigma-1} - \zeta_{s+1,\varsigma+1}\Big).
\end{aligned} \tag{11}$$

$$\begin{aligned}
\frac{\partial^2 \chi_{s,\varsigma}}{\partial \xi^2} &= \frac{6}{h^2}\Big(\zeta_{s-1,\varsigma-1} + 4\zeta_{s-1,j} + \zeta_{s-1,\varsigma+1} - 2\zeta_{s,\varsigma-1} - 8\zeta_{s,\varsigma} - 2\zeta_{s,\varsigma+1} + \zeta_{s+1,\varsigma-1} + 4\zeta_{s+1,\varsigma} + \zeta_{s+1,\varsigma+1}\Big),\\
\frac{\partial^2 \chi_{s,\varsigma}}{\partial \eta^2} &= \frac{6}{h^2}\Big(\zeta_{s-1,\varsigma-1} - 2\zeta_{s-1,\varsigma} + \zeta_{s-1,\varsigma+1} + 4\zeta_{s,\varsigma-1} - 8\zeta_{s,\varsigma} + 4\zeta_{s,\varsigma+1} + \zeta_{s+1,\varsigma-1} - 2\zeta_{s+1,\varsigma} + \zeta_{s+1,\varsigma+1}\Big),\\
\frac{\partial^2 \chi_{s,\varsigma}}{\partial \xi\, \partial \eta} &= \frac{9}{h^2}\Big(\zeta_{s-1,\varsigma-1} - \zeta_{s-1,\varsigma+1} - \zeta_{s+1,\varsigma-1} + \zeta_{s+1,\varsigma+1}\Big).
\end{aligned} \tag{12}$$

3 Time discrete scheme

For the temporal discretization, we introduce the uniform time partition $t_s = s\Delta t, \quad s = 0, 1, \ldots, N$, where $\Delta t = \frac{T}{N}$ denotes the temporal mesh size. The time derivative is approximated via the forward difference formula. We further assume that the nonlinear function $F(\chi)$ satisfies the Lipschitz condition with respect to χ, namely,

$$|F(\chi) - F(\widetilde{\chi})| \leq L|\chi - \widetilde{\chi}|, \qquad \forall\, \chi, \widetilde{\chi}, L > 0.$$

In addition, let $\Delta t \leq \frac{1}{1+L}$, and evalute (1) at the point (x, t_n) leads to

$$\frac{\chi^{n+1} - \chi^n}{\Delta t} - \frac{\Delta\chi^{n+1} - \Delta\chi^n}{\Delta t} - \Delta\chi^n + \nabla \cdot \chi^n = \nabla \cdot (F(\chi^n)) + f^n + R,$$

and $|R| < C\Delta t$, where $C > 0$. Rearranging, we obtian

$$\chi^{n+1} - \Delta\chi^{n+1} = \chi^n + (\Delta t - 1)\Delta\chi^n - \Delta t \nabla \cdot \chi^n + \Delta t \nabla \cdot (F(\chi^n)) + \Delta t f^n + \Delta t R. \tag{13}$$

We ignore R due to small value , so above equation becomes

$$\chi^{n+1} - \Delta\chi^{n+1} = \chi^n + (\Delta t - 1)\Delta\chi^n - \Delta t \nabla \cdot \chi^n + \Delta t \nabla \cdot (F(\chi^n)) + \Delta t f^n. \tag{14}$$

We now establish the convergence and stability of the discritize time scheme (1), demonstrating that it achieves a first-order convergence rate of $O(\Delta t)$.

3.1 The stability and convergence Evaluation

We investigate the stability and convergence properties of (14) using the energy method. To this end, we introduce the relevant functional spaces, equipped with their

standard norms and inner products [20] , as follows:

$$H^1(\chi) = \left\{ \chi \in L^2(\chi) : \frac{d\chi}{dx} \in L^2(\chi) \right\}, \quad \text{and} \quad H_0^1(\chi) = \left\{ \chi \in H^1(\chi) : \chi|_{\partial\chi} = 0 \right\}.$$

For $\chi, v \in L^2(\chi)$ and $\chi, v \in H^1(\chi)$, the inner products on $L^2(\chi)$ and $H^1(\chi)$ are defined, respectively, by

$$(\chi, v) = \int_\chi \chi v \, d\chi, \quad \text{and} \quad (\chi, v)_1 = (\chi, v) + (\nabla \cdot \chi, \nabla \cdot v).$$

The L^2 and H^1 norms are given by

$$\|\chi\| = (\chi, \chi)^{1/2}, \quad \|\chi\|_1 = (\chi, \chi)_1^{1/2}, \quad \text{and} \quad |\chi|_1 = (\nabla \cdot \chi, \nabla \cdot \chi)^{1/2}.$$

The weighted H^1-norm is defined [21]:

$$\|\chi\|_{w,1} = \left[\|\chi\|^2 + |\chi|_1^2 \right]^{1/2}.$$

Lemma 1 *Let $\beta_1(x)$ and $\beta_2(x)$ be any functions , so $(\nabla \cdot |\beta_1|, \beta_2) \le |\beta_1|_1 \|\beta_2\|$[11].*

Proof By definition of inner product space, we have

$$(\nabla \cdot |\beta_1|, \beta_2) = \int_\chi (\nabla \cdot |\beta_1|) \beta_2 \, d\chi$$

by using the Cauchy-Schwarz inequality [20],

$$(\nabla \cdot |\beta_1|, \beta_2) \le \left(\int_\chi (\nabla \cdot |\beta_1|)^2 \, d\chi \right)^{1/2} \left(\int_\chi \beta_2^2 \, d\chi \right)^{1/2}. \tag{15}$$

Since

$$\nabla \cdot |\beta_1| = \frac{\beta_1 (\nabla \cdot \beta_1)}{|\beta_1|}, \quad \text{and} \quad (\nabla \cdot |\beta_1|)^2 = \left(\frac{\beta_1 (\nabla \cdot \beta_1)}{|\beta_1|} \right)^2 = (\nabla \cdot \beta_1)^2.$$

So (15) becomes

$$\begin{aligned} (\nabla \cdot |\beta_1|, g) &\le \left(\int_\chi (\nabla \cdot |\beta_1|)^2 \, d\chi \right)^{1/2} \left(\int_\chi \beta_2^2 \, d\chi \right)^{1/2} = \left(\int_\chi (\nabla \cdot \beta_1)^2 \, d\chi \right)^{1/2} \left(\int_\chi \beta_2^2 \, d\chi \right)^{1/2} \\ &= |\beta_1|_1 \|\beta_2\|. \end{aligned}$$

□

Theorem 1 *The discritized time scheme given by (14) is stable in the H^1-norm [11], provided that $\Delta t \le \frac{1}{1+L}$.*

Proof. Let χ^{n+1} and $\widehat{\chi}^{n+1}$ denote the exact and approximate solutions of (14), respectively. The corresponding roundoff error can be expressed in the following form:

$$\mathfrak{E}^{n+1} - \Delta \mathfrak{E}^{n+1} = \mathfrak{E}^n + (\Delta t - 1) \Delta \mathfrak{E}^n - \Delta t \nabla \cdot \mathfrak{E}^n + \Delta t \nabla \cdot (F(\chi^n) - F(\widehat{\chi}^n)), \tag{2.7}$$

where $\mathfrak{E}^{n+1} = \chi^{n+1} - \widehat{\chi}^{n+1}$. Applying the Lipschitz condition gives

$$\mathfrak{E}^{n+1} - \Delta\mathfrak{E}^{n+1} \leq \mathfrak{E}^n + (\Delta t - 1)\Delta\mathfrak{E}^n - \Delta t\nabla\cdot\mathfrak{E}^n + \Delta tL\nabla\cdot(|\chi^n - \widehat{\chi}^n|)$$

and hence

$$\mathfrak{E}^{n+1} - \Delta\mathfrak{E}^{n+1} \leq \mathfrak{E}^n + (\Delta t - 1)\Delta\mathfrak{E}^n - \Delta t\nabla\cdot\mathfrak{E}^n + \Delta tL\nabla\cdot|\mathfrak{E}^n|. \tag{16}$$

Multiplying (16) by $\mathfrak{E}^{n+1}$ and integrating over χ, we obtain

$$\begin{aligned}\|\mathfrak{E}^{n+1}\|^2 - (\Delta\mathfrak{E}^{n+1}, \mathfrak{E}^{n+1}) \leq (\mathfrak{E}^n, \mathfrak{E}^{n+1}) + (\Delta t - 1)(\Delta\mathfrak{E}^n, \mathfrak{E}^{n+1})\\ - \Delta t(\nabla\cdot\mathfrak{E}^n, \mathfrak{E}^{n+1}) + \Delta tL(\nabla\cdot|\mathfrak{E}^n|, \mathfrak{E}^{n+1}).\end{aligned}$$

Using integration by parts,

$$\begin{aligned}\|\mathfrak{E}^{n+1}\|^2 + (\nabla\cdot\mathfrak{E}^{n+1}, \nabla\cdot\mathfrak{E}^{n+1}) \leq (\mathfrak{E}^n, \mathfrak{E}^{n+1}) - (\Delta t - 1)(\nabla\cdot\mathfrak{E}^n, \nabla\cdot\mathfrak{E}^{n+1}) + \Delta t(\mathfrak{E}^n, \nabla\cdot\mathfrak{E}^{n+1})\\ +\Delta tL(\nabla\cdot|\mathfrak{E}^n|, \mathfrak{E}^{n+1}).\end{aligned}$$

Using the Schwarz inequality and Lemma 1, we can write

$$\begin{aligned}\|\mathfrak{E}^{n+1}\|^2 + |\mathfrak{E}^{n+1}|_1^2 &\leq \|\mathfrak{E}^n\|\|\mathfrak{E}^{n+1}\| + (1 - \Delta t)|\mathfrak{E}^n|_1|\mathfrak{E}^{n+1}|_1 + \Delta t\|\mathfrak{E}^n\||\mathfrak{E}^{n+1}|_1 + \Delta tL|\mathfrak{E}^n|_1\|\mathfrak{E}^{n+1}\|\\ &\leq \frac{1}{2}\|\mathfrak{E}^n\|^2 + \frac{1}{2}\|\mathfrak{E}^{n+1}\|^2 + \left(\frac{1}{2} - \frac{\Delta t}{2}\right)\left(|\mathfrak{E}^n|_1^2 + |\mathfrak{E}^{n+1}|_1^2\right) + \frac{\Delta t}{2}\left(\|\mathfrak{E}^n\|^2 + |\mathfrak{E}^{n+1}|_1^2\right)\\ &\quad + \frac{\Delta tL}{2}\left(|\mathfrak{E}^n|_1^2 + \|\mathfrak{E}^{n+1}\|^2\right).\end{aligned}$$

By simplification of the above relation, we obtain

$$\left(\frac{1}{2} - \frac{\Delta tL}{2}\right)\|\mathfrak{E}^{n+1}\|^2 + \frac{1}{2}|\mathfrak{E}^{n+1}|_1^2 \leq \left(\frac{1}{2} + \frac{\Delta t}{2}\right)\|\mathfrak{E}^n\|^2 + \left(\frac{1}{2} - \frac{\Delta t}{2} + \frac{\Delta tL}{2}\right)|\mathfrak{E}^n|_1^2.$$

Thus,

$$(1 - \Delta tL)\|\mathfrak{E}^{n+1}\|^2 + |\mathfrak{E}^{n+1}|_1^2 \leq (1 + \Delta t)\|\mathfrak{E}^n\|^2 + (1 - \Delta t + \Delta tL)|\mathfrak{E}^n|_1^2.$$

Now, since

$$\Delta t \leq \frac{1}{1 + L},$$

we have

$$(1 - \Delta t(1 + L))\left\{\|\mathfrak{E}^{n+1}\|^2 + |\mathfrak{E}^{n+1}|_1^2\right\} \leq (1 + \Delta t(1 + L))\left\{\|\mathfrak{E}^n\|^2 + |\mathfrak{E}^n|_1^2\right\}.$$

Also, using the weighted H^1-norm, we can write

$$\|\mathfrak{E}^{n+1}\|_{\chi,1}^2 \leq q\|\mathfrak{E}^n\|_{w,1}^2,$$

and therefore

$$\begin{aligned}\|\mathfrak{E}^{n+1}\|_{w,1}^2 &\leq q^2\|\mathfrak{E}^{n-1}\|_{w,1}^2\\ &\vdots\\ &\leq q^{n+1}\|\mathfrak{E}^0\|_{w,1}^2.\end{aligned}$$

where $q = \frac{1+\Delta t(1+L)}{1-\Delta t(1+L)}$. By applying limits

$$\lim_{n\to\infty}(q)^{n+1} = \frac{e^{T(1+L)}}{e^{-T(1+L)}} = e^{2T(1+L)}.$$

Therefore,

$$\|\mathfrak{E}^{n+1}\|_{w,1} \leq \sqrt{e^{2T(1+L)}}\,\|\mathfrak{E}^0\|_{w,1}, \qquad n = 0, 1, \ldots, N-1.$$

This completes the proof. □

Theorem 2 *Let $w(x,t_n) = w^n$ and $W(x,t_n) = W^n \in H_0^1$ denote the exact and approximate solutions of Eqs. (1.1)–(1.3), respectively, satisfying the prescribed initial and boundary conditions. So, the discrete time solution converges in the H^1-norm with order $O(\Delta t)$ [11].*

Proof. By subtracting (13) and (14), we have

$$\nu^{n+1} - \Delta\nu^{n+1} = \nu^n + (\Delta t - 1)\Delta\nu^n - \Delta t\nabla\cdot\nu^n + \Delta t\nabla\cdot(F(w^n) - F(W^n)) + \Delta tR,$$

where $\nu^n = w^n - W^n$, $\quad |R| \leq C\Delta t$, $\quad \nu^0 = 0$. Using the Lipschitz condition, we get

$$\nu^{n+1} - \Delta\nu^{n+1} \leq \nu^n + (\Delta t - 1)\Delta\nu^n - \Delta t\nabla\cdot\nu^n + \Delta tL\nabla\cdot|\nu^n| + \Delta tR.$$

Multiplying the above equation by ν^{n+1} and applying the Schwarz inequality and Lemma 1 yields, after simplification,

$$\left(\frac{1}{2} - \frac{\Delta tL}{2}\right)\|\nu^{n+1}\|^2 + \frac{1}{2}|\nu^{n+1}|_1^2 \leq \left(\frac{1}{2} + \frac{\Delta t}{2}\right)\|\nu^n\|^2 + \left(\frac{1}{2} - \frac{\Delta t}{2} + \frac{\Delta tL}{2}\right)|\nu^n|_1^2 + \Delta t|R|\|\nu^{n+1}\|.$$

Using the Poincaré inequality [22],

$$\|\nu^{n+1}\| \leq C|\nu^{n+1}|_1,$$

and using the relation

$$ab \leq \frac{1}{2\theta}a^2 + \frac{\theta}{2}b^2, \qquad \forall\theta > 0,$$

we can write

$$\left(\frac{1}{2} - \frac{\Delta tL}{2}\right)\|\nu^{n+1}\|^2 + \frac{1}{2}|\nu^{n+1}|_1^2 \leq \left(\frac{1}{2} + \frac{\Delta t}{2}\right)\|\nu^n\|^2 + \left(\frac{1}{2} - \frac{\Delta t}{2} + \frac{\Delta tL}{2}\right)|\nu^n|_1^2 + \frac{\Delta t^2C^2}{2\Delta t}|R|^2 + \frac{\Delta t}{2}|\nu^{n+1}|_1^2.$$

Therefore,

$$(1-\Delta tL)\|\nu^{n+1}\|^2+(1-\Delta t)|\nu^{n+1}|_1^2 \leq (1+\Delta t)\|\nu^n\|^2+(1-\Delta t+\Delta tL)|\nu^n|_1^2+\Delta tC^2|R|^2.$$

By using the $\Delta t \leq \frac{1}{1+L}$, we get

$$(1-\Delta t(1+L))\left[\|\nu^{n+1}\|^2+|\nu^{n+1}|_1^2\right] \leq (1+\Delta t(1+L))\left[\|\nu^n\|^2+|\nu^n|_1^2\right]+\Delta tC^2|R|^2.$$

By using wegihted norm, we get

$$\|\nu^{n+1}\|_{w,1}^2 \leq q\left\{\|\nu^n\|_{w,1}^2+\Delta tC^2|R|^2\right\},$$

where $q=\frac{1+\Delta t(1+L)}{1-\Delta t(1+L)}$, then

$$\|\nu^{n+1}\|_{w,1}^2 \leq q\left\{\|\nu^n\|_{w,1}^2+\Delta tC^2|R|^2\right\}.$$

Applying the above inequality repeatedly, we obtain

$$\|\nu^{n+1}\|_{w,1}^2 \leq q^{n+1}\|\nu^0\|_{w,1}^2+\Delta tC^2|R|^2\left(q+q^2+\cdots+q^{n+1}\right).$$

Since $\nu^0=0$, we obtain

$$\|\nu^{n+1}\|_{w,1}^2 \leq \Delta tC^2|R|^2\left(q+q^2+\cdots+q^{n+1}\right).$$

Now,

$$q+q^2+\cdots+q^{n+1} \leq (n+1)q^{n+1}.$$

Hence,

$$\begin{aligned}\|\nu^{n+1}\|_{w,1}^2 &\leq \Delta t(n+1)C^2|R|^2q^{n+1}\\ &= TC^2|R|^2q^{n+1}.\end{aligned}$$

Using relation (2.10), we obtain

$$\|\nu^{n+1}\|_{w,1}^2 \leq TC^2e^{2T(1+L)}|R|^2.$$

Finally, since $|R| \leq C\Delta t$, and $|R|^2 \leq C^2\Delta t^2$.. so

$$\|\nu^{n+1}\|_{w,1}^2 \leq TC^2e^{2T(1+L)}C^2\Delta t^2.$$

Taking the square root gives

$$\|\nu^{n+1}\|_{w,1} \leq C\sqrt{TC^2e^{2T(1+L)}}\,\Delta t.$$

Thus,

$$\|\nu^{n+1}\|_{w,1} = O(\Delta t),$$

which completes the proof. □

4 Proposed Method

This section introduces the proposed numerical method for solving the problems under consideration. Consider the following nonlinear equation:

$$\chi_t - \Delta\chi_t - \nabla\cdot(\chi\nabla\chi) + \pi^2\chi^2 = f(\mathbf{x},t), \quad \mathbf{x}\in\chi, \quad t>0. \tag{17}$$

Simplification

$$\nabla\cdot(\chi\nabla\chi) = \chi\,\chi_{\xi\xi} + \chi\,\chi_{\eta\eta} + \chi_\xi^2 + \chi_\eta^2,$$

and

$$\Delta\chi_t = (\chi_{\xi\xi} + \chi_{\eta\eta})_t.$$

Hence the strong form can be written as:

$$\chi_t - (\chi_{\xi\xi} + \chi_{\eta\eta})_t - \chi\,\chi_{\xi\xi} - \chi\,\chi_{\eta\eta} - \chi_\xi^2 - \chi_\eta^2 + \pi^2\chi^2 = f.$$

Applying fnite difference for time descritization and the θ-scheme equation (4) becomes

$$\begin{aligned}&\frac{\chi^{n+1}-\chi^n}{\Delta t} - \frac{(\chi_{\xi\xi}^{n+1}+\chi_{\eta\eta}^{n+1}) - (\chi_{\xi\xi}^{n}+\chi_{\eta\eta}^{n})}{\Delta t} - \theta\left[(\chi\,\chi_{\xi\xi})^{n+1} + (\chi\,\chi_{\eta\eta})^{n+1} + (\chi_\xi^2)^{n+1} + (\chi_\eta^2)^{n+1} - \pi^2(\chi^2)^{n+1}\right]\\ &= -(1-\theta)\left[(\chi\,\chi_{\xi\xi})^{n} + (\chi\,\chi_{\eta\eta})^{n} + (\chi_\xi^2)^{n} + (\chi_\eta^2)^{n} - \pi^2(\chi^2)^{n}\right] + f^{n+1}.\end{aligned} \tag{18}$$

Multiplying by Δt gives

$$\begin{aligned}&\chi^{n+1} - \chi^n - \left[\chi_{\xi\xi}^{n+1} + \chi_{\eta\eta}^{n+1} - \chi_{\xi\xi}^{n} - \chi_{\eta\eta}^{n}\right] - \Delta t\,\theta\left[(\chi\,\chi_{\xi\xi})^{n+1} + (\chi\,\chi_{\eta\eta})^{n+1} + (\chi_\xi^2)^{n+1} + (\chi_\eta^2)^{n+1} - \pi^2(\chi^2)^{n+}\right.\\ &= -\Delta t(1-\theta)\left[(\chi\,\chi_{\xi\xi})^{n} + (\chi\,\chi_{\eta\eta})^{n} + (\chi_\xi^2)^{n} + (\chi_\eta^2)^{n} - \pi^2(\chi^2)^{n}\right] + \Delta t\,f^{n+1}.\end{aligned} \tag{19}$$

Therefore,

$$\begin{aligned}&\chi^{n+1} - (\chi_{\xi\xi}^{n+1}+\chi_{\eta\eta}^{n+1}) - \Delta t\,\theta\Big[(\chi\,\chi_{\xi\xi})^{n+1} + (\chi\,\chi_{\eta\eta})^{n+1} + (\chi_\xi^2)^{n+1} + (\chi_\eta^2)^{n+1} - \pi^2(\chi^2)^{n+1}\Big]\\ &= \chi^n - (\chi_{\xi\xi}^{n}+\chi_{\eta\eta}^{n}) + \Delta t(1-\theta)\Big[(\chi\,\chi_{\xi\xi})^{n} + (\chi\,\chi_{\eta\eta})^{n} + (\chi_\xi^2)^{n} + (\chi_\eta^2)^{n} - \pi^2(\chi^2)^{n}\Big] + \Delta t\,f^{n+1}.\end{aligned} \tag{20}$$

The nonlinear terms are approximated using the following formulas:

$$(\chi\,\chi_{\xi\xi})^{n+1} \approx \chi^{n+1}\chi_{\xi\xi}^{n} + \chi^{n}\chi_{\xi\xi}^{n+1} - \chi^{n}\chi_{\xi\xi}^{n}.$$

Similarly,

$$\begin{aligned}(\chi\,\chi_{\eta\eta})^{n+1} &\approx \chi^{n+1}\chi_{\eta\eta}^{n} + \chi^{n}\chi_{\eta\eta}^{n+1} - \chi^{n}\chi_{\eta\eta}^{n}.\\ (\chi_\xi^2)^{n+1} &\approx 2\chi_\xi^n\chi_\xi^{n+1} - (\chi_\xi^n)^2.\\ (\chi_\eta^2)^{n+1} &\approx 2\chi_\eta^n\chi_\eta^{n+1} - (\chi_\eta^n)^2.\\ (\chi^2)^{n+1} &\approx 2\chi^n\chi^{n+1} - (\chi^n)^2.\end{aligned}$$

Thus, the final linearized equation is

$$\chi^{n+1} - \Delta t\,\theta\left(\chi^n_{\xi\xi} + \chi^n_{\eta\eta} - 2\pi^2\chi^n\right)\chi^{n+1} - 2\Delta t\,\theta\left(\chi^n_{\xi}\chi^{n+1}_{\xi} + \chi^n_{\eta}\chi^{n+1}_{\eta}\right) - (1+\Delta t\,\theta\chi^n)\left(\chi^{n+1}_{\xi\xi} + \chi^{n+1}_{\eta\eta}\right)$$
$$= \chi^n - \chi^n_{\xi\xi} - \chi^n_{\eta\eta} + \Delta t\,(1-2\theta)\left[\chi^n\left(\chi^n_{\xi\xi} + \chi^n_{\eta\eta}\right) + (\chi^n_{\xi})^2 + (\chi^n_{\eta})^2 - \pi^2(\chi^n)^2\right] + \Delta t\,f^{n+1}. \tag{21}$$

To approixmate the soluion by Bi-cubic B-spline at the collocation points $\{(\xi_s, \eta_\varsigma)\}^m_{s,\varsigma}$, the approximation is defined as:

$$\chi(\xi,\eta,t) = \sum_{s=-1}^{m+1}\sum_{\varsigma=-1}^{m+1}\zeta_{s\varsigma}(t)\Phi_{s\varsigma}(\xi,\eta). \tag{22}$$

The bove expression in a more compact form can be expressed as:

$$\chi^n = \mathbf{\Phi}\boldsymbol{\zeta}^n, \tag{23}$$

where $\mathbf{\Phi} = \Phi_{s\varsigma}$ is the spline matrix and $\boldsymbol{\zeta}^n$ is the coloumn matrix of the unknown coefficients to be computed. Using spline matrix for the scheme defined in ((21)) and some manipulation, we obtian in compact form as:

$$\mathbf{A}\boldsymbol{\zeta}^{n+1} = \mathbf{B}\boldsymbol{\zeta}^n + \mathbf{F}, \tag{24}$$

where

$$\mathbf{A} = \mathbf{A_{ij}} = \Phi(\mathbf{x}) - \Delta t\,\theta\left(\chi^n_{xx} + \chi^n_{\eta\eta} - 2\pi^2\chi^n(\mathbf{x})\right) * \Phi(\mathbf{x}) - 2\Delta t\,\theta\left(\chi^n_x * \Phi_\xi(\mathbf{x}) + \chi^n_\eta * \Phi_\eta(\mathbf{x})\right)$$
$$- (1+\Delta t\,\theta\chi^n(\mathbf{x})) * \left(\Phi_{\xi\xi}(\mathbf{x}) + \Phi_{\eta\eta}(\mathbf{x})\right),$$

where $*$ means the element wise multiplication and $\mathbf{x} = (\xi,\eta)$. Similerly, one can express $\mathbf{B}$ and $\mathbf{F}$. Using (23) and (27), we obtain the solution

$$\chi^{n+1} = \mathbf{\Phi}\mathbf{A}^{-1}\mathbf{B}\mathbf{\Phi}^{-1}\chi^n + \mathbf{\Phi}\mathbf{A}^{-1}\mathbf{F} \tag{25}$$

For $n = 0$, equation (27) becomes

$$\mathbf{A}\boldsymbol{\zeta}^1 = \mathbf{B}\boldsymbol{\zeta}^0 + \mathbf{F}, \tag{26}$$

First we compute $\boldsymbol{\zeta}^0$ from the initial conditions and after one can compute the unknowns for arbitrary time level together with bounary conditions and hence the solution can be obtinaed from equtaion (28).

5 Stability Analysis

In this section, we apply matrix method to analysis the stability of the given scheme. Thus, express (27) as:

$$\boldsymbol{\zeta}^{n+1} = \mathbf{A}^{-1}\mathbf{B}\boldsymbol{\zeta}^n + \mathbf{A}^{-1}\mathbf{F}, \tag{27}$$

and

$$\chi^{n+1} = \mathbf{\Phi A}^{-1}\mathbf{B\Phi}^{-1}\chi^{n} + \mathbf{\Phi A}^{-1}\mathbf{F} \tag{28}$$

Let e be the error and defined as:

$$e = U - \chi \tag{29}$$

where U and χ describle exact and approximate solutions, respectively. The corresponding error vector then satisfies the following relation:

$$e^{n+1} = \mathcal{H}e^{n}, \forall n \geq 0, \tag{30}$$

where $\mathcal{H} = \mathbf{\Phi A}^{-1}\mathbf{B\Phi}^{-1}$ is the damping factor. Using matrix method stability, if $\|\mathcal{H}\| \leq 1$, the scheme is stable. In addition, it obeys that the condition $\nu(\mathcal{H}) \leq 1$ since $\nu(\mathcal{H}) \leq \|\mathcal{H}\|$.

6 Test Problems

This section applies the proposed numerical method to some test problems to evaluate its accuracy and effectiveness. For individual problem, the numerical results are compared with the corresponding exact solution and previously published results. The $\mathfrak{E}_2$ and $\mathfrak{E}_\infty$ norms are expressed as:

$$\mathfrak{E}_2 = \sqrt{\sum_{s=1}^{M+1}\sum_{r=1}^{M+1}(\chi - U)^2}, \qquad \mathfrak{E}_\infty = \max_{1\leq s,r\leq 2M}|\chi - U|. \tag{5.1}$$

where χ and U be the approximate and exact solutions, respectively.
Example 6.1. We begin with the following linear Sobolev equation: [1]:

$$\chi_t - \Delta\chi_t - \Delta\chi = f(\mathbf{x}), \qquad \mathbf{x} \in \chi,\ t > 0. \tag{31}$$

The exact solution is given by

$$\chi(\mathbf{x}, t) = \sin(\pi\xi)\sin(\pi\eta)e^{-t} \tag{32}$$

The corresponding initial conditions, boundary conditions, and source terms are obtained from the exact solutions. The approximate solution is considered in the domian $\chi = [0, 1]\times[0, 1]$ and tomporal domian $[0, 1]$. We compute solution for different values of N and Δt in the form of error norms and display the results in Tables 1–3. From Table 1, it is abvous that the result of present method better than [1, 2]. Furthermore, the results are computed for different values of temporal mesh size in Table 2 with additon of different spatial numbers in Table 3. By decreasing of mesh sizes, the error reduces which clearly show the convergence. In comparison with [10], present method give better results. Figure 1 illustrates the convergence behavior in both space and time, whereas Figure 2 displays the solution profiles along with their

absolute errors. As shown in the figure, the exact and approximate solutions exhibit strong agreement, remaining very close to one another.

Table 1: Numerical errors at $t = 1$, using $\Delta t = 0.01$ and $\theta = \frac{1}{2}$.

	Present Method		[1]		[2]	
N	$\mathfrak{E}_2$	$\mathfrak{E}_\infty$	$\mathfrak{E}_2$	$\mathfrak{E}_\infty$	$\mathfrak{E}_2$	$\mathfrak{E}_\infty$
4×4	6.03730E-04	8.4438E-04	1.7519E-02	7.4767E-03	8.0968E-03	2.2100E-02
8×8	3.35061E-04	4.3848E-04	8.9465E-03	2.1515E-03	2.9283E-03	6.4901E-03
16×16	1.74709E-04	2.2799E-04	4.0019E-03	4.9543E-04	8.0121E-04	1.7223E-03
32×32	8.85418E-05	1.1704E-04	9.5508E-04	5.9549E-05	1.9983E-04	4.2893E-04

Table 2: Comparison of the error norms at $T = 1$ and $M = 16$.

	Present Method		[10]	
Δt	$\mathfrak{E}_2$	$\mathfrak{E}_\infty$	$\mathfrak{E}_2$	$\mathfrak{E}_\infty$
1/10	1.44415×10^{-4}	2.9825×10^{-4}	1.5645×10^{-4}	3.1325×10^{-4}
1/20	3.60760×10^{-5}	7.4506×10^{-5}	3.7653×10^{-5}	7.6267×10^{-5}
1/40	9.01727×10^{-6}	1.8623×10^{-5}	9.2546×10^{-6}	1.8810×10^{-5}
1/80	2.25421×10^{-6}	4.6555×10^{-6}	3.0341×10^{-6}	5.8740×10^{-6}
1/160	5.63546×10^{-7}	1.1639×10^{-6}	6.6410×10^{-6}	2.2108×10^{-5}
1/320	1.40886×10^{-7}	2.90966×10^{-7}	2.5270×10^{-6}	1.6881×10^{-5}

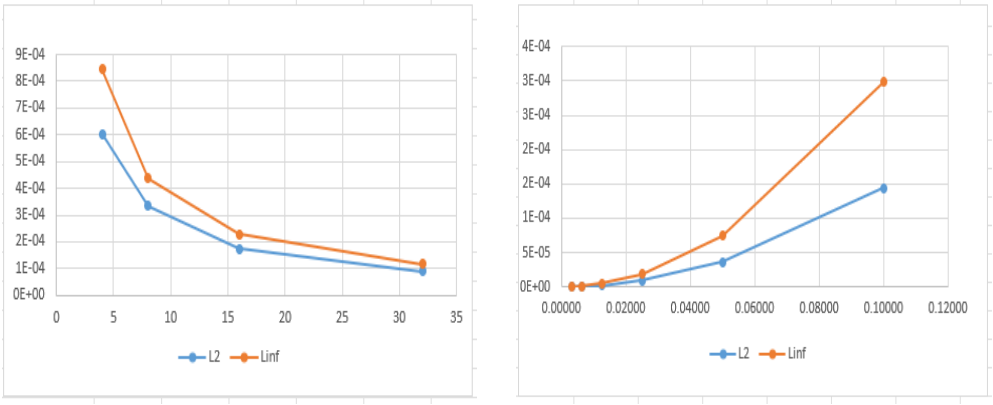
Example 6.2. Consider the problem is given by

$$\chi_t - \Delta\chi_t - \Delta\chi = f(\mathbf{x}), \qquad \mathbf{x} \in \chi,\ t > 0. \tag{33}$$

subject to exact solution is given by

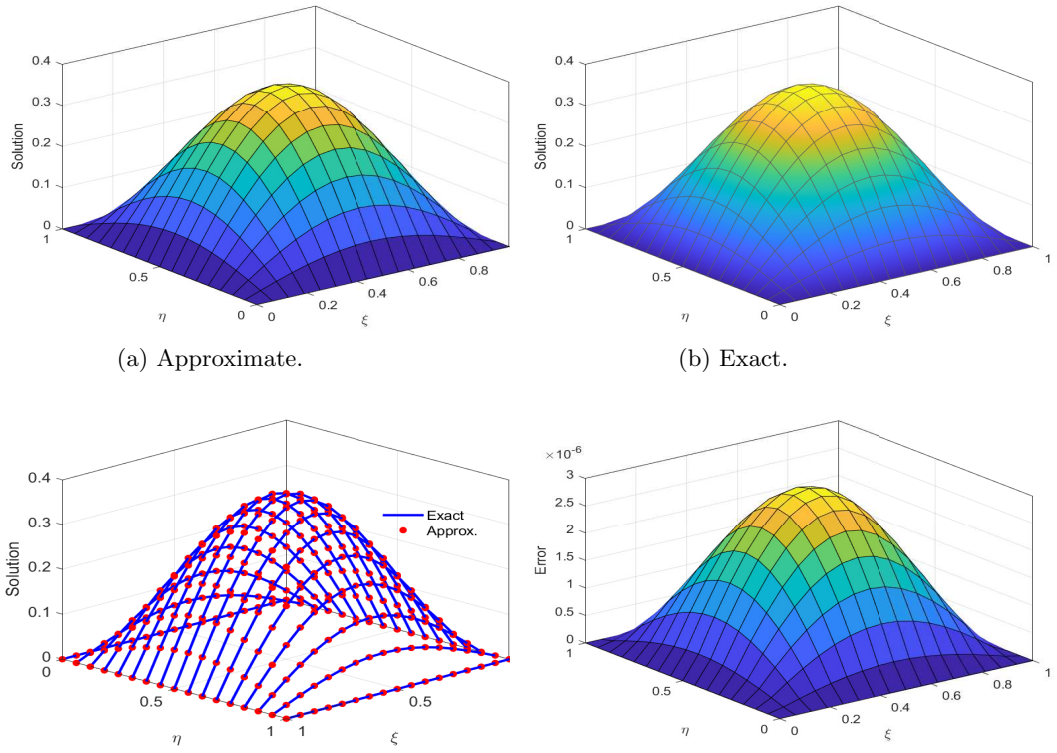
$$\chi(\mathbf{x}, t) = \sin(\pi\xi)\sin(\pi\eta)e^{\xi-\eta-t}. \tag{34}$$

All conditions such as initial, boundary and sourse term are derived from (34). We consider spatial domain $\chi = [0, 1] \times [0, 1]$ and temporal domian $[0, 1]$. We calculte solution for different values of N and Δt in the form of error norms and presents the findings in Tables 4–6. From Table 4, it is observed that the results of proposed method better than [1, 2, 10]. In Table 5–6, $\mathfrak{E}_2$ and $\mathfrak{E}_\infty$ norms are calculated for different values of mesh and collocation points. By decreasing of mesh sizes, the error reduces



(a) Collocation point vs Error (b) Time step vs Error.

Fig. 1: Comparison of error with respect to space points and temporal step size.



(a) Approximate. (b) Exact.

(c) Pointwise comparison. (d) Error.

Fig. 2: Graphs of χ at $N = 16$, $\Delta t = 0.01$ and plot at final time level.

Table 3: Error profile for different values of N and Δt at the final time for Example 1.

		Present Method		[10]	
Δt	N	$\mathfrak{E}_2$	$\mathfrak{E}_\infty$	$\mathfrak{E}_2$	$\mathfrak{E}_\infty$
1/20	4×4	2.70167E-05	6.1785E-05	1.6403E-03	2.2512E-03
1/40	10×10	8.54189E-06	1.8002E-05	1.7776E-05	3.5907E-05
1/80	15×15	2.24095E-06	4.5847E-06	3.9467E-05	1.0697E-04
1/160	20×20	5.73509E-07	1.1767E-06	4.9066E-06	1.6893E-05

which clearly show the convergence. Also from comparion in Tables5–6, the proposed method provides better result than [10]. Figure 3 displays the solution profiles along with their absolute errors and plot of exact and approximate at final time level.

Table 4: Comparison of the error norms for different N, $\Delta t = 0.001$, and $\theta = 1/2$ at the final time level.

	Present Method		[10]		[1]		[2]	
N	$\mathfrak{E}_2$	$\mathfrak{E}_\infty$	$\mathfrak{E}_2$	$\mathfrak{E}_\infty$	$\mathfrak{E}_2$	$\mathfrak{E}_\infty$	$\mathfrak{E}_2$	$\mathfrak{E}_\infty$
4×4	7.22795E-04	1.3876E-03	2.8829E-03	6.7457E-03	1.0450E-02	6.2773E-03	1.2651E-03	5.2085E-03
8×8	4.05183E-04	7.2630E-04	3.0982E-04	5.4484E-04	5.9420E-03	1.7252E-03	4.2776E-04	1.6720E-03
16×16	2.12144E-04	3.8568E-04	2.8012E-04	5.3827E-04	2.6154E-03	3.8947E-04	1.1685E-04	4.5449E-04
32×32	1.07777E-04	2.0070E-04	2.7821E-04	5.3604E-04	6.8838E-04	4.9551E-05	2.9622E-05	1.1697E-04

Example 6.3. The problem is governed by the following nonlinear Sobolev equation

$$\chi_t - \Delta\chi_t - \nabla \cdot (\chi \nabla \chi) + \pi^2 \chi^2 = f, \qquad \mathbf{x} \in \chi, \quad t > 0, \tag{5.4}$$

together with the prescribed initial and boundary conditions

$$\begin{cases} \chi(\mathbf{x}, 0) = \sin(\pi\xi)\sin(\pi\eta), & \mathbf{x} \in \chi, \\ \chi(\mathbf{x}, t) = e^t \sin(\pi\xi)\sin(\pi\eta), & \mathbf{x} \in \partial\chi, \quad t > 0. \end{cases} \tag{35}$$

The corresponding source function is

$$\begin{aligned} f(\mathbf{x}, t) = & -e^{2t}\pi^2 \cos^2(\pi\xi)\sin^2(\pi\eta) - e^{2t}\pi^2 \sin^2(\pi\xi)\cos^2(\pi\eta) \\ & + e^t \sin(\pi\xi)\sin(\pi\eta) + 2e^t\pi^2 \sin(\pi\xi)\sin(\pi\eta) \\ & + 3e^{2t}\pi^2 \sin^2(\pi\xi)\sin^2(\pi\eta). \end{aligned} \tag{36}$$

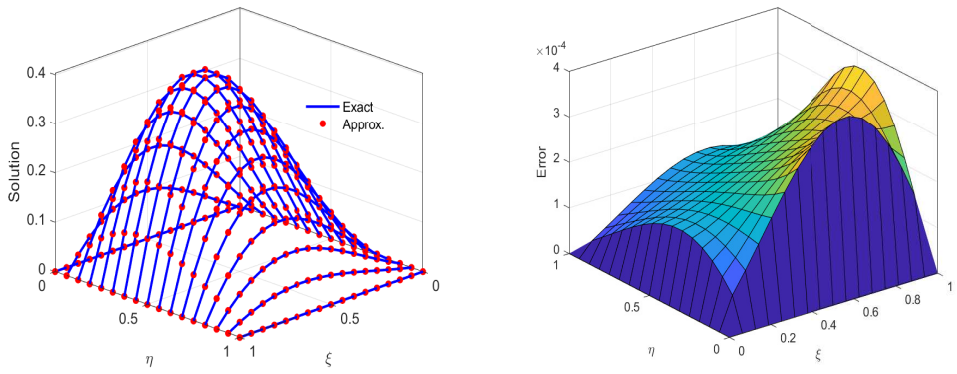
$$\chi(\mathbf{x}, t) = e^t \sin(\pi\xi)\sin(\pi\eta). \tag{37}$$

Table 5: Assessment of the error for various values of Δt at $T = 1$ in Example 2.

	Present Method		[10]	
Δt	$\mathfrak{E}_2$	$\mathfrak{E}_\infty$	$\mathfrak{E}_2$	$\mathfrak{E}_\infty$
1/10	2.10083E-03	3.9750E-03	5.0660E-04	1.0345E-03
1/20	1.05566E-03	1.9540E-03	3.7230E-04	7.3303E-04
1/40	5.29367E-04	9.6894E-04	3.3810E-04	6.4224E-04
1/80	2.65095E-04	4.8249E-04	3.2494E-04	6.0748E-04
1/160	1.32654E-04	2.4076E-04	3.1280E-04	5.8564E-04
1/320	6.63541E-05	1.20256E-04	3.1136E-04	5.8034E-04
1/640	3.31839E-05	6.00974E-05	3.0640E-04	5.6980E-04

Table 6: Error profile at $M = 16$ and $T = 1$ in Example 2.

		Present Method		[10]	
Δt	N	$\mathfrak{E}_2$	$\mathfrak{E}_\infty$	$\mathfrak{E}_2$	$\mathfrak{E}_\infty$
1/20	4×4	3.66477E-03	7.0484E-03	2.8457E-03	6.5725E-03
1/40	10×10	8.27817E-04	1.4941E-03	3.2085E-04	6.1925E-04
1/80	15×15	2.82035E-04	5.1364E-04	3.0822E-04	5.8149E-04
1/160	20×20	1.06988E-04	1.9593E-04	2.8014E-04	5.7743E-04



(a) Pointwise comparison. (b) Exact solution.

Fig. 3: Approximate solution, exact solution, pointwise comparison, and absolute error for Example 5.2 at $t = 1$.

The corresponding boundary conditions are obtained from the exact solutions. The consideration of interval of spatial and time domian are $\chi = [0,1] \times [0,1]$ and $[0,1]$. Error norms in the form of L_2 and L_∞ are computed in Table 7, it is abvous that the result of present method better than [1, 3, 7]. Furthermore, the results are evaluated for different values of temporal mesh size in Table 8 with additon of different spatial numbers in Table 9. By decreasing of mesh sizes, the error reduces which clearly show the convergence. In comparison with [10], proposed method gives better results. Figure 4 illustrates the solution profiles along with their absolute errors. As shown in the figure, the exact and approximate solutions show strong agreement to one another.

Table 7: Errors analysis for different values of N, with $\Delta t = 0.001$, $\theta = 1$, and $t = 1$.

	Present method		[1]		[3]	
N	$\mathfrak{E}_2$	$\mathfrak{E}_\infty$	$\mathfrak{E}_\infty$	$\mathfrak{E}_2$	$\mathfrak{E}^2(L^2)$	$\mathfrak{E}^2(H^1)$
4	3.23016E−02	6.8375E−02	5.8662E−02	1.7284E−01	3.1576E−02	7.2335E−01
8	9.26724E−03	1.7303E−02	1.3147E−02	7.5881E−02	7.8313E−03	3.6045E−01
16	2.37155E−03	4.2163E−03	3.0030E−03	3.4724E−02	1.9572E−03	1.8008E−01
32	4.97887E−04	8.7232E−04	5.5208E−04	1.3063E−02	–	–

Table 8: Comparison of error norms for different vlaues of $\Delta t, N = 16$ at $T = 1$ in Example 4.

	Present method		[10]	
dt	$\mathfrak{E}_2$	$\mathfrak{E}_\infty$	$\mathfrak{E}_2$	$\mathfrak{E}_\infty$
1/10	7.03999E−03	1.3279E−02	1.6876E−01	1.4301E−01
1/20	4.94274E−03	7.4381E−03	8.1577E−02	6.8945E−02
1/40	3.73220E−03	4.7022E−03	4.0199E−02	3.3883E−02
1/80	3.09919E−03	4.6696E−03	2.0074E−02	1.6855E−02
1/160	2.78642E−03	4.5844E−03	1.0299E−02	6.5175E−03
1/320	2.63395E−03	4.52463E−03	5.7292E−03	4.5076E−03

Example 6.4. The problem is governed by the nonlinear generalized Benjamin-Bona-Mahony-Burgers (NGBBMB) equation

$$\chi_t - \Delta\chi_t - \Delta\chi + \nabla \cdot \chi = \chi\chi_\xi + \chi\chi_\eta + f, \qquad \mathbf{x} \in \chi, \quad t > 0, \tag{5.10}$$

along with initial and boundary conditions

$$\begin{cases} \chi(\mathbf{x}, 0) = 0, & \mathbf{x} \in \chi, \\ \chi(\mathbf{x}, t) = t\sin(\xi + \eta), & (\mathbf{x} \in \partial\chi, \quad t > 0. \end{cases} \tag{38}$$

Table 9: Comparison of error norms for different value of N and $\Delta t = 0.01$at $T = 1$ in Example 4.

		Present method		[10]	
dt	N	$\mathfrak{E}_2$	$\mathfrak{E}_\infty$	$\mathfrak{E}_2$	$\mathfrak{E}_\infty$
1/20	4×4	4.18134E−02	7.2998E−02	5.2244E−02	6.9198E−02
1/40	10×10	8.08892E−03	1.1968E−02	4.5109E−02	3.3871E−02
1/80	15×15	3.46939E−03	5.2742E−03	2.7432E−02	1.6574E−02
1/160	20×20	1.85270E−03	2.9583E−03	1.0582E−02	8.3523E−03

$$f(\mathbf{x}, t) = \left[3 + t - 2t^2 \cos(\xi + \eta)\right] \sin(\xi + \eta) + t \cos(\xi + \eta). \tag{39}$$

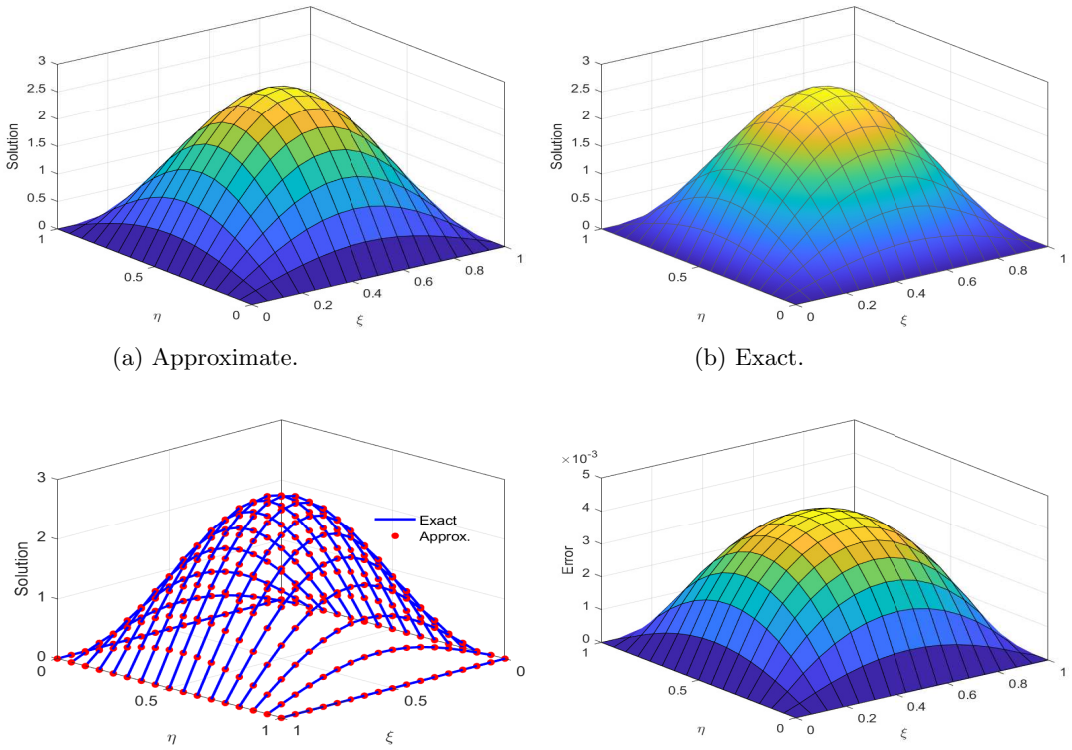
The corresponding initial conditionsand boundary conditions are obtained from the exact solutions. The approximate solution is calculated in the domian $\chi = [0, 1] \times [0, 1]$ and tomporal domian $[0, 1]$. We compute solution for different values of N and Δt in the form of error norms and display the results in Tables 10–11. From Table 10, it is abvous that the result of present method better than [1]. Furthermore, the results are obtained for different values of temporal mesh size in Table 11. By decreasing of mesh sizes, the error reduces which clearly show the convergence. In comparison with [1, 11], present method give better results. Figure 5 displays the solution profiles along with their absolute errors. As shown in the figure, the exact and approximate solutions exhibit strong agreement, remaining very close to one another.

Table 10: Comparison of error norms for different values of N, $\Delta t = 0.01$, $\theta = 1/2$ at final time level.

t	Present results		[1]	
	$\mathfrak{E}_\infty$	$\mathfrak{E}_2$	$\mathfrak{E}_\infty$	$\mathfrak{E}_2$
0.1	2.0555×10^{-4}	9.68732×10^{-5}	9.7897×10^{-5}	9.0478×10^{-4}
0.2	2.0575×10^{-4}	9.90565×10^{-5}	2.0530×10^{-4}	1.9331×10^{-3}
0.5	2.0628×10^{-4}	1.05188×10^{-4}	5.6699×10^{-4}	5.2227×10^{-3}
1.0	2.0709×10^{-4}	1.14308×10^{-4}	9.8933×10^{-4}	8.5980×10^{-3}

7 Conclusion

This study presented a numerical method based on bicubic spline interpolation for solving the (1+2)-dimensional Sobolev and GBBMB equations. The proposed hybrid approach combines finite-difference approximations with bicubic splines to transform the governing PDEs into systems of algebraic equations that can be solved efficiently. Several test problems were examined to assess the accuracy and performance of the scheme using the $\mathfrak{E}_2$ and $\mathfrak{E}_\infty$ error norms. The numerical results demonstrated excellent agreement with the exact solutions and previously reported results. Moreover, the graphical comparisons further confirmed the accuracy, reliability, and effectiveness of the proposed method.



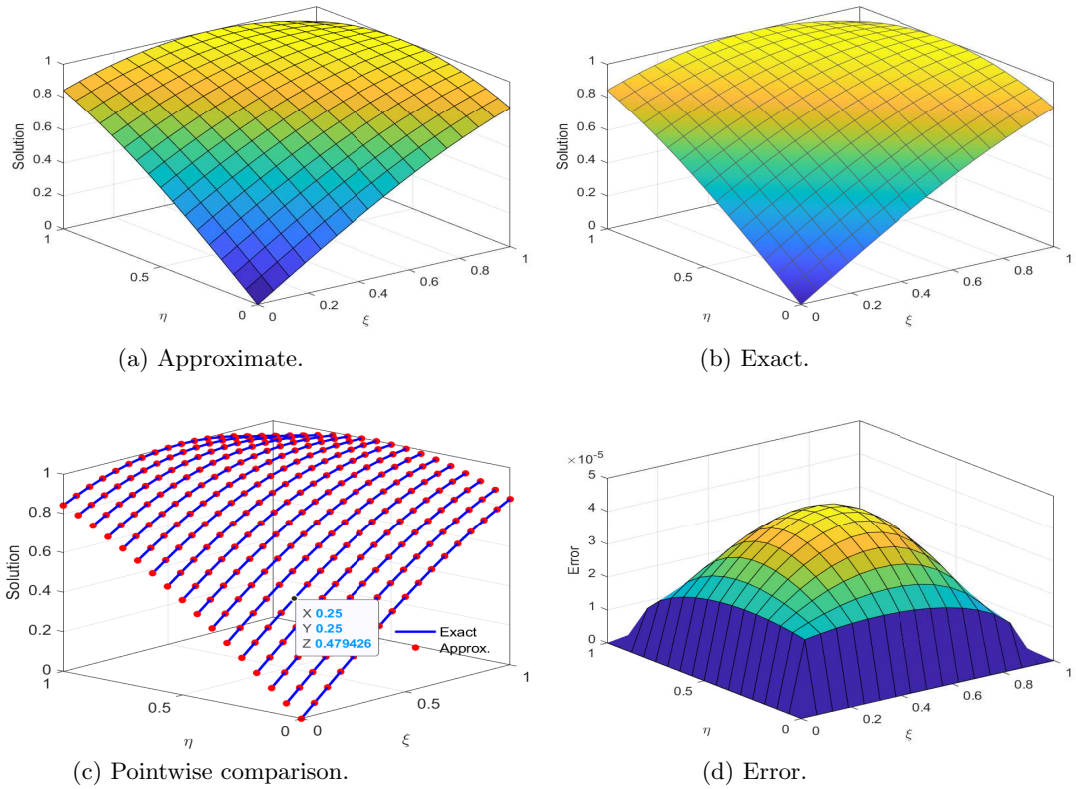
(a) Approximate. (b) Exact.

(c) Pointwise comparison. (d) Error.

Fig. 4: Graphs of χ at $h = 1/16, \Delta t = 0.01$ and plot at final time level.

Table 11: comparision of resutls for different time mesh size at $N = 16$ and $t = 1$.

Δt	Present results		[11]		[1]	
	$\mathfrak{E}_\infty$	$\mathfrak{E}_2$	$\mathfrak{E}_\infty$	$\mathfrak{E}_2$	$\mathfrak{E}_\infty$	$\mathfrak{E}_2$
1/10	3.2728×10^{-3}	1.62000×10^{-3}	6.7487×10^{-3}	2.6698×10^{-2}	4.1369×10^{-3}	1.0243×10^{-2}
1/20	1.6356×10^{-3}	8.10723×10^{-4}	2.6171×10^{-3}	1.0355×10^{-2}	2.4115×10^{-3}	5.8698×10^{-3}
1/40	8.1936×10^{-4}	4.17592×10^{-4}	1.1038×10^{-3}	4.6405×10^{-3}	1.5207×10^{-3}	3.6346×10^{-3}
1/80	4.1179×10^{-4}	2.24546×10^{-4}	4.6863×10^{-4}	2.0854×10^{-3}	1.0682×10^{-3}	2.5188×10^{-3}
1/160	2.1048×10^{-4}	1.29915×10^{-4}	2.0224×10^{-4}	9.4879×10^{-4}	8.4022×10^{-4}	1.9708×10^{-3}
1/320	1.35193×10^{-4}	8.42686×10^{-5}	8.9161×10^{-5}	4.3993×10^{-4}	7.2574×10^{-4}	1.7034×10^{-3}
1/640	1.07454×10^{-4}	6.28277×10^{-5}	4.0189×10^{-5}	2.0868×10^{-4}	6.7980×10^{-4}	1.5724×10^{-3}
1/1280	9.61598×10^{-5}	5.2936×10^{-5}	1.8510×10^{-5}	1.0151×10^{-4}	6.6576×10^{-4}	1.5079×10^{-3}
1/2560	9.05194×10^{-5}	4.83468×10^{-5}	8.9827×10^{-6}	5.1444×10^{-5}	6.5874×10^{-4}	1.4759×10^{-3}



(a) Approximate.

(b) Exact.

(c) Pointwise comparison.

(d) Error.

Fig. 5: Graphs of χ at $h = 1/16, \Delta t = 0.01$ and plot at final time level.

Declaration

Data Availability

The data used to support the findings of this study are available from the corresponding author upon request.

Funding

Not applicable.

Conflicts of Interests

The authors declare that they have no conflict of interest.

References

[1] Haq, S., Ghafoor, A.: Numerical solutions of two dimensional sobolev equations. Computers & Mathematics with Applications **77**, 565–575 (2019)

[2] Gao, F., Wang, X.: A modified weak galerkin finite element method for sobolev equation. Journal of Computational Mathematics, 307–322 (2015)

[3] He, S., Li, H., Liu, Y.: Time discontinuous galerkin space-time finite element method for nonlinear sobolev equations. Frontiers of Mathematics in China **8**(4), 825–836 (2013)

[4] Zhang, Q., Gao, F.: A fully-discrete local discontinuous galerkin method for convection-dominated sobolev equation. Journal of Scientific Computing **51**(1), 107–134 (2012)

[5] Gu, H.: Characteristic finite element methods for nonlinear sobolev equations. Applied Mathematics and Computation **102**(1), 51–62 (1999)

[6] Sun, T., Yang, D.: The finite difference streamline diffusion methods for sobolev equations with convection-dominated term. Science Direct Working Paper (S1574-0358), 04 (2001)

[7] Gao, F., Cui, J., Zhao, G.: Weak galerkin finite element methods for sobolev equation. Journal of Computational and Applied Mathematics **317**, 188–202 (2017)

[8] Peregrine, D.H.: Calculations of the development of an undular bore. Journal of fluid mechanics **25**(2), 321–330 (1966)

[9] Oruç, Ö.: A computational method based on hermite wavelets for two-dimensional sobolev and regularized long wave equations in fluids. Numerical Methods for Partial Differential Equations **34**(5), 1693–1715 (2018)

[10] Haq, S., Ali, I.: Approximate solution of two-dimensional sobolev equation using a mixed lucas and fibonacci polynomials. Engineering with Computers **38**(Suppl 3), 2059–2068 (2022)

[11] Dehghan, M., Abbaszadeh, M., Mohebbi, A.: The numerical solution of nonlinear high dimensional generalized benjamin–bona–mahony–burgers equation via the meshless method of radial basis functions. Computers & Mathematics with Applications **68**(3), 212–237 (2014)

[12] Ganji, Z., Ganji, D., Bararnia, H.: Approximate general and explicit solutions of nonlinear bbmb equations by exp-function method. Applied Mathematical Modelling **33**(4), 1836–1841 (2009)

[13] Hamid, N.N.A., Majid, A.A., Ismail, A.I.M.: Bicubic b-spline interpolation

method for two-dimensional heat equation. In: AIP Conference Proceedings, vol. 1682 (2015). AIP Publishing

[14] Abd Hamid, N.N., Abd. Majid, A., Md. Ismail, A.I.: Bicubic b-spline interpolation method for two-dimensional laplace's equations. In: AIP Conference Proceedings, vol. 1522, pp. 1033–1038 (2013). American Institute of Physics

[15] Arshad, A., Mittal, R., Sharma, S.: An efficient scheme for solution of two-dimensional laplace's equation. In: Conference on Applied Mathematics and Computational Sciences (ICAMCS-2019) (2019)

[16] Motiun, C.N., Sulaiman, J., Janteng, A., Supriatna, A.K.: A bicubic b-spline approximation and application of c-bseg methods for the solution of 2d elliptic partial differential equations. Edelweiss Applied Science and Technology **9**(11), 710–725 (2025)

[17] Raslan, K., Ali, K.K.: A new structure formulations for cubic b-spline collocation method in three and four-dimensions. Nonlinear Engineering **9**(1), 432–448 (2020)

[18] Gardner, L., Gardner, G.: A two dimensional bi-cubic b-spline finite element: used in a study of mhd-duct flow. Computer methods in applied mechanics and engineering **124**(4), 365–375 (1995)

[19] De Boor, C., De Boor, C.: A Practical Guide to Splines vol. 27. springer New York, ??? (1978)

[20] Kreyszig, E.: Introductory Functional Analysis with Applications. John Wiley & Sons, ??? (1991)

[21] Zhang, N., Deng, W., Wu, Y.: Finite difference/element method for a two-dimensional modified fractional diffusion equation. Advances in Applied Mathematics and Mechanics **4**(4), 496–518 (2012)

[22] Quarteroni, A., Valli, A.: Numerical Approximation of Partial Differential Equations. Springer, ??? (1994)